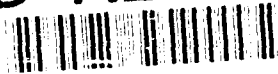


AD-A237 499



MIL IR 91-18

AD

# EFFECT OF HYDROGEN ON THE ELECTRONIC STRUCTURE OF A GRAIN BOUNDARY IN IRON

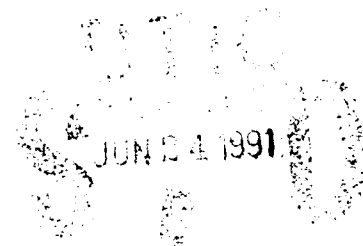
GENRICH L. KRASKO

U.S. ARMY MATERIALS TECHNOLOGY LABORATORY  
METALS RESEARCH BRANCH

GREGORY B. OLSON

NORTHWESTERN UNIVERSITY  
DEPARTMENT OF MATERIALS SCIENCE AND ENGINEERING, EVANSTON, IL

May 1991



Approved for public release; distribution unlimited.



US ARMY  
LABORATORY COMMAND  
MATERIALS TECHNOLOGY LABORATORY

91-03057



U.S. ARMY MATERIALS TECHNOLOGY LABORATORY  
Watertown, Massachusetts 02172-0001

SECURITY CLASSIFICATION OF THIS PAGE (When Data Entered)

DU 1 JAN 73 1473

UNCLASSIFIED

SECURITY CLASSIFICATION OF THIS PAGE (When Data Entered)

Block No. 20

# ABSTRACT

Linear Muffin-Tin Orbitals-Atomic Sphere Approximation (LMTO-ASA) calculations were performed on a 26-atom supercell model of a  $\Sigma 3$  (111) grain boundary (GB) in bcc Fe. The supercell emulated two GBs with 11 (111) planes of Fe atoms between the GB planes. One of the GBs was clean, with a structural vacancy at the GB core in the center of a trigonal prism of Fe atoms, while on the other GB this site was occupied by an H atom. The interplanar spacings of the supercell were relaxed using a modified embedded atom method. As in the case of P and S in a similar GB environment in Fe, there is only a weak interaction between H and the nearest Fe atoms. Almost all the Fe d-states are nonbonding. A very weak covalent bond exists between H and Fe due to s-pd hybridization; the hybrid bonding band located far below the Fermi energy ( $E_F$ ). This bond is mostly of  $\sigma$ -type, connecting H with the Fe atoms in the GB plane; the  $\delta$ -component of this bond across the GB is weaker. Contrary to a general belief, H on the GB does not contribute any significant electron charge to Fe valence d-bands. A weak electrostatic interaction attracts Fe-atoms across the clean GB, but results in repulsion if an H atom is present. The magnetic contribution to intergranular cohesion is decreased when H is present due to the suppression of the magnetic moments of the nearest Fe atoms both in the GB plane and directly across the GB.

## INTRODUCTION

The reduced cohesion of grain boundaries (GB) is often the controlling factor limiting the ductility of high strength metallic alloys.<sup>1</sup> This is particularly so when there is an environmental interaction, as in the case of intergranular hydrogen stress corrosion cracking.<sup>2</sup> Typically, hydrogen drastically degrades mechanical properties of metal alloys, making them unreliable and poses a significant technological problem.

Intergranular embrittlement in metals is usually associated with prior segregation of impurities toward the GBs.<sup>3-6</sup> Impurities present in bulk concentrations of  $10^{-3}$ - $10^{-4}$  atomic percent can result in a dramatic decrease in plasticity. The hydrogen concentration is also extremely low; its solid solubility in bcc Fe below room temperature is only 1 ppm ( $10^{-4}$  atomic percent).<sup>7</sup>

Previous studies attempted to explain GB decohesion on the electron-atom level due to hydrogen by using small atomic clusters as a simple model of GB.<sup>8</sup> Decohesive effects of hydrogen were also successfully investigated using semiempirical calculations and modelling<sup>9</sup> based upon the Embedded Atom Method (EAM).<sup>10</sup> It was shown that a single hydrogen atom in a unit cell at a GB of fcc Ni can weaken the metallic bonds across the GB lowering the fracture stress by 15%.

Progress in developing efficient first-principles methods in the recent decade has allowed more detailed treatments of a GB with an impurity. Calculations making use of both two-dimensional<sup>11,12</sup> and supercell<sup>13</sup> models have provided a deeper insight into the mechanisms of impurity decohesion.

The effect of hydrogen on the electronic structure of transition metals has also been a focus of numerous research papers<sup>14</sup> mainly directed at an investigation of stable hydrides. However, since Fe does not form a compound with hydrogen, neither hydrogen in the bulk Fe nor in Fe GB has been studied in detail thus far.

The present paper reports preliminary results of the self-consistent, spin-polarized calculations of the electronic structure of H in an atomic environment typical of a GB in Fe. A more detailed analysis will be reported at a later date.

Atomistic relaxation studies<sup>15</sup> have shown that an interstitial impurity atom, such a boron, is likely to occupy the center of a capped trigonal prism formed by Fe atoms in the core of the GB. Hydrogen, due to its small atomic size, may possibly occupy tetrahedral voids in the GB plane rather than centers of trigonal prisms. In the present study, however, H has been treated in the same way as B, C, P, and S atoms in the Fe GB.<sup>13</sup>

A 26-atom supercell was used as a model of the GB (see Figure 1) with the corresponding crystal lattice viewed as a succession of hexagonal planes with stacking:

...BABCBABCABCACBACBACBACBAB...

Accession For	
NTIS GRA&I	<input checked="" type="checkbox"/>
DTIC TAB	<input type="checkbox"/>
Unannounced	<input type="checkbox"/>
Justification	
By	
Distribution/	
Availability Codes	
Avail and/or	
Dist	
A-1	

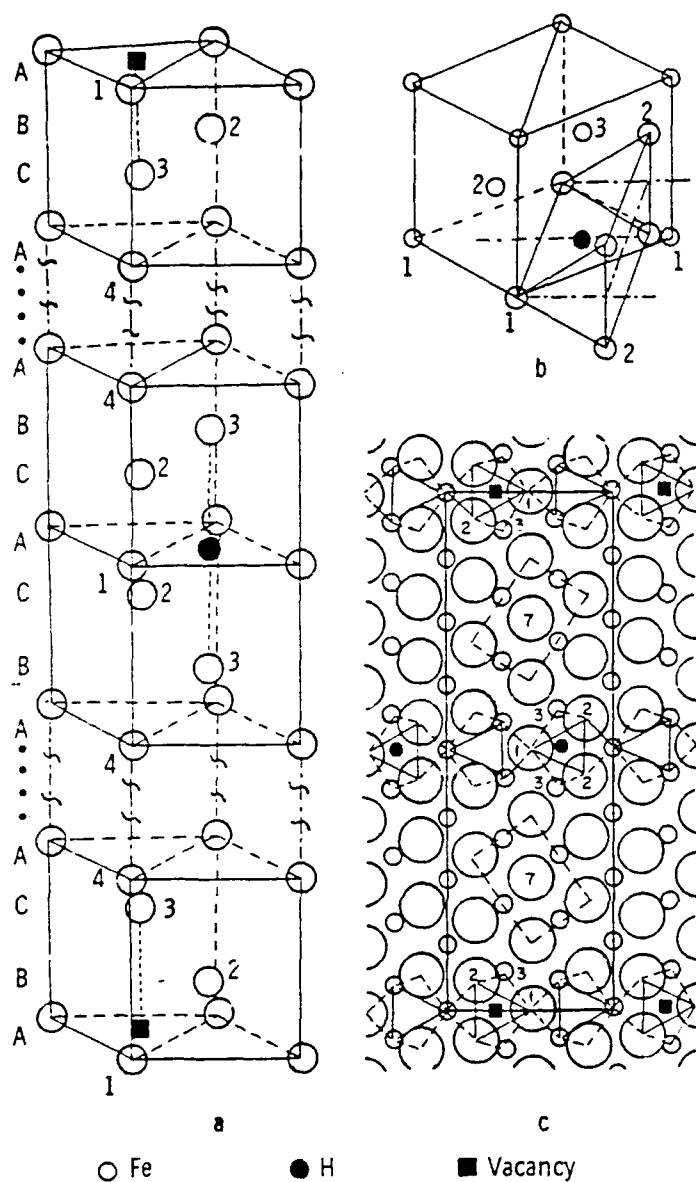


Figure 1. 26-atom supercell model of GB. a) The hexagonal supercell; only parts of the unit cell adjacent to the GB are shown. b) The trigonal prism environment on the GB planes. c) View along [112] direction of the periodic (111) plane array; small and large circles are Fe atoms in alternating (110) planes. The capped trigonal prisms on the GB are shown. The broken line rectangles centered at Fe-7 atoms show the projections of bcc unit cells.

The two stacking faults, ...BAB... and ...CAC..., imitate two (111)  $\Sigma 3$  tilt GB. One of the GBs is occupied by an H atom, while the other is "clean;" an empty sphere (ES) is placed inside the trigonal prism of Fe atoms (see filled square in Figure 1). There are 11 planes of Fe atoms between the two GB planes (A). It is important that information on both the clean GB and the GB with H can be obtained within the same calculation. In order to find the energy difference resulting from placing an H atom on the GB, an independent reference calculation on a supercell with two clean GBs was also performed.

To make the GB model more realistic, both the clean GB and that with H were "relaxed" by minimizing energy as a function of interplanar spacings. The Finnis-Sinclair<sup>16</sup> version of EAM was used; the energy of an H atom was found as a function of local electron charge

density at the H-site due to surrounding Fe atoms from the so-called Effective Medium Theory (EMT).<sup>17</sup>

Spin-polarized scalar-relativistic calculations were done using the Linear Muffin-Tin Orbitals (LMTO) method.<sup>18,19</sup> The exchange-correlation functional of von Barth and Hedin<sup>20</sup> and the frozen core approximation were used.

## RESULTS AND DISCUSSION

Figure 2 shows the relaxed interplanar distances for both the clean GB and the GB with H. An interesting feature of the clean GB is that the distance between the second and third planes is only half of the (111) interplanar distance in bulk bcc Fe. The consequences of this feature will be discussed below.

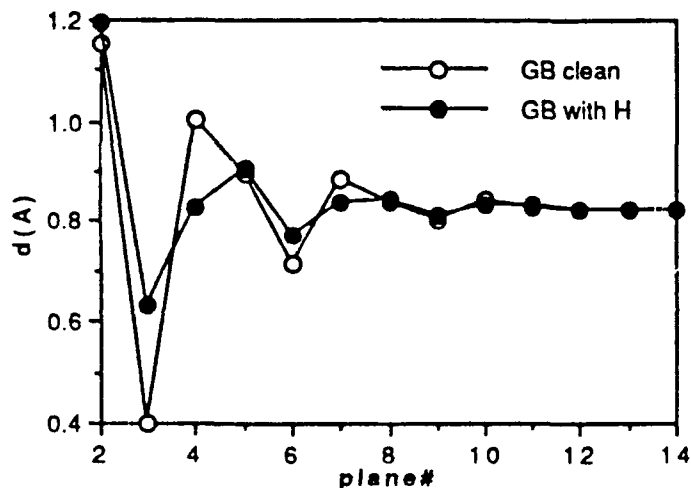


Figure 2. "Relaxed" distances between (111) GB planes number  $i$  and  $i-1$  for the clean GB, and GB with hydrogen as a function of the plane number  $i$ . The GB plane is plane 1; atoms Fe-1 belong to plane 1, Fe-2 to plane 2, etc..

Figures 3 and 4 show the electronic densities of states (DOS) in units of states/Ry versus energy in mRy. The zero of energy corresponds to the Fermi energy ( $E_F$ ) of perfect bcc Fe. The arrows show the  $E_F$  for the clean GB and GB with H.

In Figure 3 we compare the DOS of a bulk bcc Fe atom with the site-projected DOS of atom Fe-7 on the central plane between the two GBs. The two DOS plots are very much alike, which suggests that the supercell size is sufficient for minimal interaction of the two GBs. It is observed, however, that the d-bands of the Fe-7 atom are somewhat narrowed, since the distances between Fe-7 and its neighbors are slightly increased due to the "tail" of the elastic "relaxation wave;" the latter "dumps out" only after 13 to 15 crystal planes from the GB (see Figure 2).

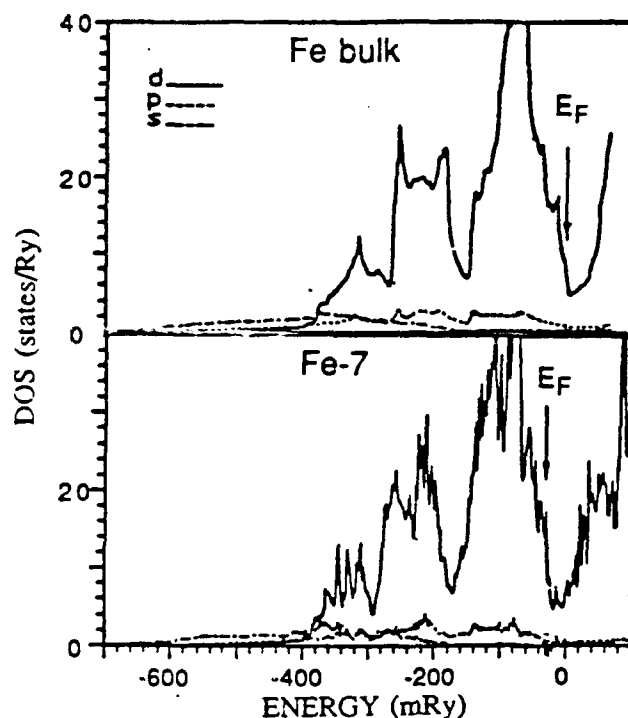


Figure 3. DOS for the bulk bcc Fe atom (upper plot) and Fe-7 (center) atom in the supercell (lower plot).

Figures 4a through 4c compare the site-projected DOS for atoms Fe-1, Fe-2, and Fe-3 for the clean GB (upper plots) and the GB with H (lower plot). The bottom ("negative") parts of the lower plots show the site-projected DOS within the Wigner-Seitz (WS) sphere of the H atom. These DOS are identical for the three plots.

The DOS of the Fe-1 atom on the clean GB is strongly distorted compared to that for a bulk atom. This can be easily understood since relaxation of the clean GB brings the (111) planes of the Fe-2 and Fe-3 atoms very close to each other as we mentioned above (the interplanar distance is only 0.407Å, compared to 0.825Å in the bulk). It is only the interaction of the Fe-3 plane with the outer planes Fe-4, Fe-5, and Fe-6 which prevents it from collapsing into an  $\omega$ -phase configuration. In fact, the DOS for the Fe-1 atom on the clean GB, as shown in Figure 4a, is very much like the DOS for the  $\omega$ -phase.<sup>21</sup> Off the GB plane, in Fe-2 and Fe-3, the DOS acquire more bcc-like features.

The presence of H on the GB pushes the Fe-2 and Fe-3 planes apart making the Fe-1 DOS more bcc-like. In Fe-2 and Fe-3 the bcc shape is further restored. The d-band width behaves as one could have expected; i.e., following the lattice distortion pattern, being in general, narrower on the GB with H. A number of peaks around  $E_F$  on both the GBs are characteristic of localized GB states.

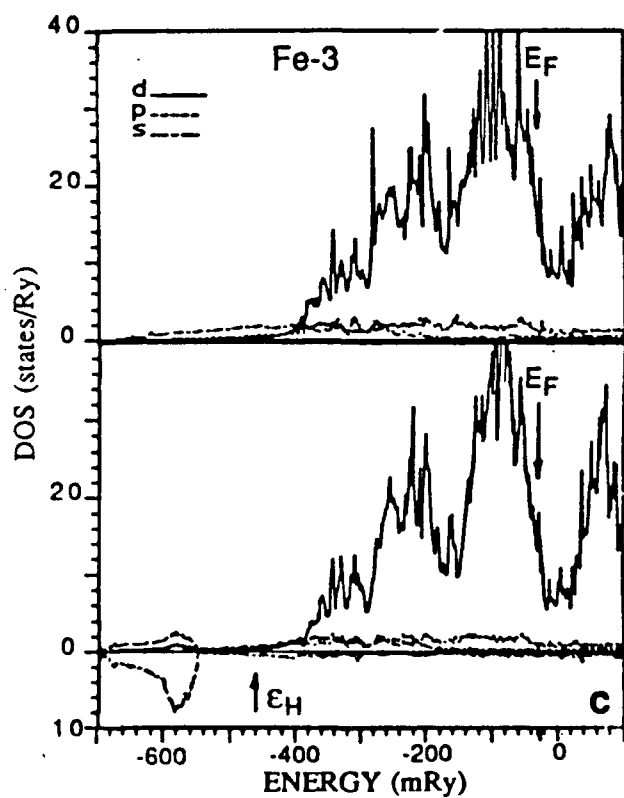
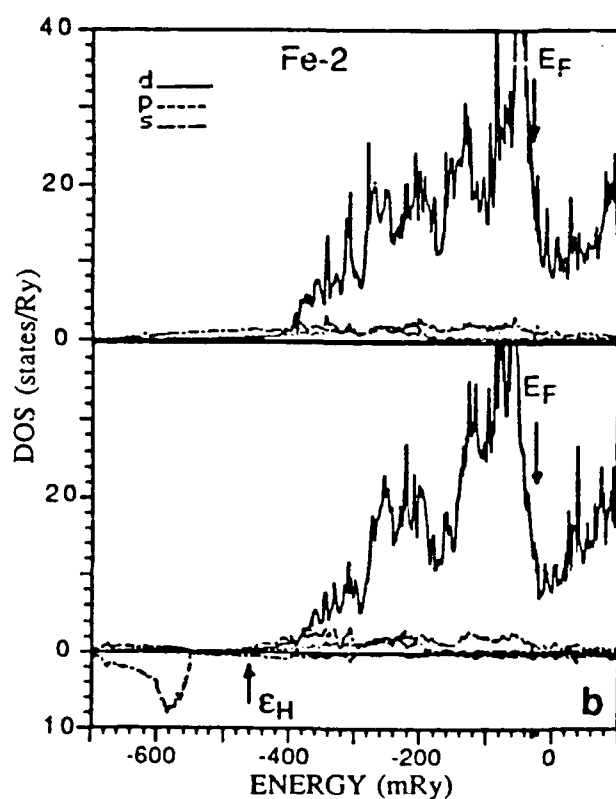
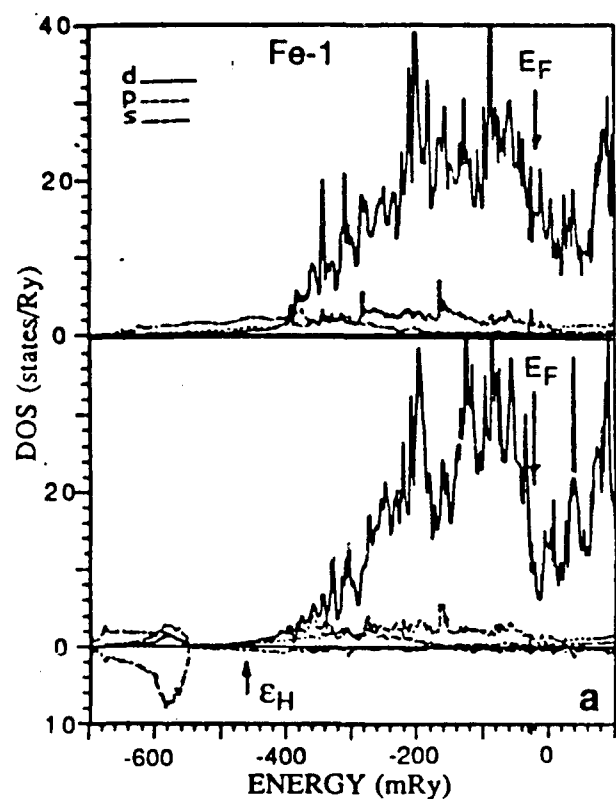


Figure 4 a-c. The site-projected DOS for atoms Fe-1, Fe-2, and Fe-3 for the clean GB (upper plots) and the GB with H (lower plots). The bottom ("negative") parts of the lower plots show the site-projected DOS within the WS sphere of the H atom (same for the three plots).



When H is placed on the iron GB, Fe-H chemical bonds are formed, as in the case of other impurities.<sup>13</sup> These are the consequence of electron hybridization. Since the ground state of the electron in an isolated H atom ( $\epsilon_H$  in Figures 4a through 4c) corresponds to an energy range where the Fe pd-components are extremely weak, only a weak s-pd hybridization can be expected. The latter results in forming a bonding band, with states of mostly s-type within the WS sphere of H, and of mostly pd-type in the WS spheres of the Fe atoms.\* A simple estimate shows that an antibonding component of the hybrid should appear in the energy range about (-160 to -180) mRy. In fact, one can see a series of tiny peaks superimposed on the "bcc-like" dip in the DOS plots in this energy range. Unlike a more typical case when impurity antibonding states are located above  $E_F$ , these antibonding states are filled, thus resulting in a decrease of stability.

The strongest bonding d-component is localized on the Fe-1 atoms even though the Fe-3 atom is closer to the H site; the numbers of d-electrons in these states are 0.069 and 0.045, respectively. This indicates that the s-d hybrid's  $\sigma$ -component spreading out in the GB plane is stronger than a  $\delta$ -component, penetrating across the GB.

A question of importance is what happens with the H electron? It has been generally believed<sup>3,14,22</sup> that in group 7 and 8 transition metals H donates its electron to a host's valence d-band. The results of Reference 13 for the Fe GB with B, C, P, and S showed there was a strong charge redistribution among the atomic spheres, but the present results show that this is not the case for H. Table 1 presents the total numbers of electrons,  $n$ , within atomic WS spheres ( $s_0$  are the sphere radii in a.u.), their s-, p-, and d-components, and the magnetic moments,  $m$  (in  $\mu_B$ /atom). Though the concept of charge transfer is quite ambiguous, nevertheless, some of the features of the charge redistribution pattern shall be discussed.

Since the WS radii of the Fe atoms of "relaxed" GB with and without H are different, it is difficult to compare the contents of s- and p- electrons in the corresponding WS spheres. Comparison of the d-electron numbers is more meaningful, since the d-states are more localized, and the d-electron content should not be sensitive to the WS radii. It can be seen from Table 1 that upon placing H on the GB the number of electrons localized on Fe-1, Fe-2, and Fe-3 atoms increase, respectively, by 0.186, 0.027, and 0.010 electrons/atom. The calculations show that the numbers of d-electrons localized in the impurity bonding bands are 0.069, 0.030, and 0.045, respectively; then, the numbers of d-electrons in the "valence" part of the spectrum changes by +0.117, -0.003, and -0.035. Thus, the total change in the d-electron content per H atom (based upon 1Fe-1, 2Fe-2, and 2Fe-3 atoms per each H atom on the GB, as shown in Figure 1) is 0.260, of which 0.217 d-electrons are localized in the Fe bonding bands, while the valence d-band population increases by only 0.041 electron. At the same time, there is a "deficiency" of 0.238 electrons in the WS sphere of the H atom.

\*As for the s-components of the Fe impurity bands, they are merely "tails" of the s-electron distribution in the Hydrogen WS sphere.

Table 1.

Atom	$s_0$	$n_s$	$n_p$	$n_d$	$n$	$m$
■	0.753	0.045	0.004	0.000	0.049	0.002
Fe-1	2.834	0.727	0.935	6.689	8.350	2.595
Fe-2	2.519	0.593	0.638	6.490	7.722	2.043
Fe-3	2.654	0.625	0.732	6.572	7.929	2.339
Fe-4	2.790	0.721	0.919	6.694	8.335	2.387
Fe-7	2.661	0.615	0.730	6.505	7.849	2.340
bcc, bulk	2.661	0.641	0.784	6.575	8.000	2.298
Fe-4	2.778	0.710	0.888	6.664	8.262	2.395
Fe-3	2.617	0.614	0.710	6.582	7.907	2.097
Fe-2	2.588	0.620	0.649	6.518	7.788	2.232
Fe-1	2.961	0.761	0.992	6.875	8.628	2.501
H	1.326	0.697	0.059	0.006	0.762	-0.017

In spite of the ambiguity of charge transfer, the atomic sphere approximation (ASA) used in the LMTO method enables one to draw meaningful conclusions regarding electrostatic interactions at the GB. Our calculations show (see Table 1) that the change in net sphere charges upon placing the H atom on the GB changes the electrostatic interaction between the spheres. On the clean GB, the electronic charge localized within the ES has an electrostatic repulsion with the excess charge on Fe-1 and attraction with the charge deficient Fe-2 and Fe-3. Thus, the Fe-3 atoms across the GB are pulled towards each other by their attraction to the ES. On the other hand, on the GB with H, due to the electronic deficiency in the H sphere, there is an attraction between H and Fe-1, and repulsion between H and Fe-2 and Fe-3. Thus, the Fe-3 atoms across the GB undergo repulsion from each other.

Finally, a few words about the effect of H on the ferromagnetic moment,  $m$  (in  $\mu_B/\text{atom}$ ), of the nearby Fe atoms. First of all, the enhancement of  $m$  (2.595) of the Fe-1 atom on the clean GB plane with respect to that of the center Fe-7 atom (2.340), or the bcc bulk atom (2.298), is similar to that expected around a two-dimensional defect. Enhancement of  $m$  on Fe free surfaces has been consistently predicted.<sup>23,24</sup> Similar to the case of the free surface, the origin of the moment enhancement in GB is the emergence of the localized GB states in the d-component of the DOS at  $E_F$ . This enhancement is slightly weakened (2.501) upon adding an H atom to the GB, possibly due to the narrowing of the d-band and thus decreasing the d-DOS at  $E_F$ . A more considerable suppression of  $m$  is found for the Fe-3 atom (2.097 versus 2.339 on the clean GB). The moment on the Fe-2 atoms is only slightly enhanced. As for the H atom, it appears to have a very low  $m$  (0.0173), due to spin polarization of s-electrons, antiferromagnetically coupled to the Fe magnetic moments.

## CONCLUSIONS

It has been found that in a typical Fe GB environment, hydrogen has a very weak bonding with the iron atoms both in the GB plane and across the GB; the latter being relatively weaker than the former. A weak electrostatic interaction and a suppression of ferromagnetic moments of the iron atoms across the GB also contribute to decohesion. The analysis of the d-charge redistribution showed that, contrary to a general belief, hydrogen on the GB gives a negligible contribution of electron charge to the iron valence d-bands. These results should be important for understanding the decohesion mechanisms which can produce hydrogen embrittlement in iron and iron-base alloys.

## ACKNOWLEDGMENTS

This research is a part of the multi-institutional Steel Research Group (SRG) program. Research at Northwestern University is sponsored by the Office of Naval Research (ONR). The author acknowledges fruitful discussions with Dr. R. J. Harrison of the U. S. Army Materials Technology Laboratory (MTL). The author is also grateful to Dr. R. P. I. Adler and Dr. M. Azrin of MTL for their interest and support. The LMTO code developed by Professor N. Christensen has been used in all calculations.

## REFERENCES

1. BRIANT, C. L., and BANERJEE, S. K. *Embrittlement of Engineering Alloys*. C. L. Briant and S. K. Banerjee, eds., Acad. Press, New York, NY, 1983, p. 21; also, GUTTMANN, M., and McLEAN, D. *Interfacial Segregations*. W. C. Johnson and J. M. Blakey, eds., ASM, Metals Park, OH, 1979, p. 261.
2. *The Theory of Stress Corrosion Cracking in Alloys*. J. C. Scully, ed., NATO, Brussels, Belgium 1971; also, *Effect of Hydrogen on Behavior of Materials*. A. W. Thomson and L. M. Bernstein, eds., A.I.M.E., New York, NY, 1976; also, *Stress Corrosion Cracking and Hydrogen Embrittlement of Iron Base Alloys*. R. W. Staehle, J. Hockmann, R. D. McCright, and J. E. Slater, eds., NACE-5, Houston, TX, 1977; also, *Hydrogen Degradation of Ferrous Alloys*. R. N. Oriani, J. P. Hirsh, and M. Smalowski, eds., Noyes, Park Ridge, NJ, 1985.
3. TROLANO, A. R. Trans. Am. Soc. Met., v. 52, no. 54, 1960.
4. STARK, J. P., and MARCUS, H. L. Metall. Trans. A, v. 8A, no. 1425, 1977; also, LEE, D. Y., BARRERA, E. V., STARK, J. P., and MARCUS, H. L. Metall. Trans. A, v. 15A, no. 1415, 1984.
5. MEYERS, C. L., Jr., ONODA, G. Y., LEVY, A. V., and KOTHLA, R. J. Trans. Metall. Society of A.I.M.E., v. 233, no. 720, 1965.
6. SEAH, M. P. J. Phys. F, v. 10, no. 1013, 1980.
7. MCLELLAN, R. B., and COLDWELL, D. W. Acta Metall., v. 23, no. 57, 1975.
8. EBERHART, M. E., JOHNSON, F. H., and LATANISION, R. M. Acta Metall., v. 32, no. 955, 1984; also, EBERHART, M. E., LATANISION, R. M., and JOHNSON, K. H., *ibid.*, v. 33, no. 1769, 1985.
9. DAW, M. S. and BASKES, M. I. Phys. Rev. Lett., v. 50, no. 1285, 1983; also, DAW, M. S., and BASKES, M. I. *Chemistry and Physics of Fracture*. R. H. Jones and R. M. Latanision, eds., Martinus Nijhoff, 1987, p. 196.
10. DAW, M. S. Phys. Rev., v. B39, no. 7441, 1989; also, DAW, M. S., and BASKES, M. I., *ibid.*, v. B29, no. 6443, 1984.
11. HASHIMOTO, M., ISHIDA, Y., YAMAMOTO, R., DOYAMA, M., and FUJIWARA, T. J. Phys. F, v. 11, no. 1141, 1981; also, Surface Sci., v. 144, no. 182, 1984; also, HASHIMOTO, M., ISHIDA, Y., WAKAYAMA, S., YAMAMOTO, R., DOYAMA, M., and FUJIWARA, T. Acta Met., v. 32, no. 13, 1984.
12. CRAMPIN, S., VVEDENSKY, D. D., MACLAREN, J. M., and EBERHART, M. E. Phys. Rev., v. B40, no. 3413, 1989.
13. KRASKO, G. L., and OLSON, G. B. Solid State Commun., v. 76, no. 247, 1990.
14. For references see C. D. Gelatt, Jr., H. Ehrenreich, and J. A. Weiss. Phys. Rev., v. B17, no. 1940, 1978.
15. HASHIMOTO, M., ISHIDA, Y., YAMAMOTO, R., DOYAMA, M., and FUJIWARA, T. Scripta Met., v. 16, no. 267, 1982; also, HASHIMOTO, M., ISHIDA, Y., YAMAMOTO, R., and DOYAMA, M. Acta Met., v. 32, no. 1, 1984; also, ISHIDA, Y., and MORI, M., Journal de Physique, Colloque C4, v. 46, no. C4-465, 1985.
16. FINNIS, M. W., and SINCLAIR, J. E. Phil. Mag., v. A50, no. 45, 1984; v. A53, no. 161, 1986.
17. NØRSKOV, J. K. Phys. Rev., v. B26, no. 2875, 1982.
18. ANDERSEN, O. K., JEPSEN, O., and GLÖTZEL, D. *Highlights of Condensed Matter Theory*. F. Bassani, F. Fumi, and M. P. Tosi, eds., North Holland, NY, 1985; also, ANDERSEN, O. K. *Electronic Structure of Complex Systems*. P. Phariseau, and W. M. Timmerman, eds., Plenum Press, New York, NY, 1984, p. 11.
19. SKRIVER, H. L. *The LMTO Method*. Springer, Berlin, Germany, 1984.
20. VON BARTH, U., and HEDIN, L. J. Phys., v. C5, no. 1629, 1972.
21. SIKKA, S. K., VOHRA, Y. K., and CHIDAMBARAM, R. *Progress in Materials Science*. J. W. Christian, P. Haasen, and T. B. Massalski, eds., Pergamon Press, New York, NY, v. 27, 1982, p. 245.
22. KRONMÜLLER, H. *Hydrogen in Metals I*. G. Alefeld, and J. Völkl, eds., Springer, Berlin, Germany, 1978.
23. WANG, G. S., and FREEMAN, A. F. Phys. Rev., v. B24, no. 4364, 1981; also, OHNISHI, S., and FREEMAN, A. F., *ibid.*, v. B28, no. 671, 1983.
24. KRASKO, G. L., and OLSON, G. B. *Innovations in Ultrahigh-Strength Steel Technology*. G. B. Olson, M. Azrin, and F. S. Wright, eds., Sagamore Army Materials Research Conference Proceedings, Lake George, NY, v. 34, Aug. 30 - Sept. 3, 1987, p. 677.